Ultrafast vibrational dynamics of doubly hydrogen bonded acetic acid dimers in liquid solution

ARTICLE *in* CHEMICAL PHYSICS LETTERS · JANUARY 2001

Impact Factor: 1.9 · DOI: 10.1016/S0009-2614(00)01384-1

12 January 2001

ELSEVIER

Chemical Physics Letters 333 (2001) 248–254

CHEMICAL PHYSICS LETTERS

www.elsevier.nl/locate/cplett

Ultrafast vibrational dynamics of doubly hydrogen bonded acetic acid dimers in liquid solution

G. Seifert *, T. Patzlaff, H. Graener

Martin-Luther-Universität Halle-Wittenberg, Fachbereich Physik/Fachgruppe Optik, Hoher Weg 8, D-06099 Halle, Germany

Received 20 September 2000; in final form 2 November 2000

Abstract

Acetic acid dimers in liquid CCl_4 have been studied by picosecond infrared double resonance spectroscopy in the 2000 to 3800 cm^{-1} region. A subpicosecond redistribution of the vibrational energy among the various modes within the broad OH band of the hydrogen-bonded dimer ring was found; an effective vibrational lifetime of 4.0 ± 1.5 ps was measured for the whole ensemble. The additionally observed slower decay component of 15 ps is attributed to nanoscopic thermal diffusion and the reaction of the hydrogen bond system to the elevated temperature. © 2001 Elsevier Science B.V. All rights reserved.

1. Introduction

Carboxylic acid molecules have been known for a long time to form rather stable hydrogen-bonded dimers both in the gas phase and in liquid solution [1,2]. The rather complicated infrared and Raman spectra of, particularly, dimers of formic and acetic acid have been the subject of various experimental [3,4] and theoretical [5–7] investigations since about 1970. However, only few time-resolved experimental investigations of the picosecond vibrational and structural dynamics of this type of molecule have been published up to now; in particular the C–O stretching mode of acetic acid in liquid solution [8] and a Langmuir film of stearic acid on water [9] have been studied. In this Letter we report infrared double resonance experiments using picosecond pulses of acetic acid dimers in liquid solution, focussing on the vibrational and structural dynamics of the doubly hydrogen-bonded dimer ring and the thermalization of the excess energy. The behavior of the hydrocarbon chains will be discussed in a forthcoming paper for larger molecules such as stearic acid.

2. Experimental

All results reported below were obtained on liquid mixtures of acetic acid (purest reagent available from Merck) and CCl_4 (Aldrich). The experiments were performed at room temperature, the sample length for the transient data being 100 μm. Conventional IR spectra were taken with a Perkin–Elmer FTIR 1760 spectrometer.

The infrared double resonance spectrometer used for the present investigation has been described in detail recently [10,11]. In short, the experimental setup is based on a Kerr-lens mode-locked, flashlamp-pumped, 70 Hz Nd:YLF-laser

* Corresponding author. Fax: +49-345-55-27-221.
E-mail address: g.seifert@physik.uni-halle.de (G. Seifert).

0009-2614/01/$ - see front matter
PII: S0009-2614(00)01384-1

system ($\lambda = 1047$ nm), followed by second harmonic-pumped KTP optical parametric generators and fundamental-pumped difference frequency parametric amplifiers to produce separately tunable infrared pump and probe pulses. The tuning range is 2.5–4 μm using $LiNbO_3$ crystals in the OPAs, and 3.5–5 μm using $AgGaS_2$ crystals; a crystal change makes a realignment of the experiment necessary, so it is normally not possible to use the whole tuning range in a single scan. The pulses have typically 2.5 ps temporal and 8–10 cm^{-1} spectral width (FWHM) and energies of 30 μJ (pump pulses) and clearly below 1 μJ (probe pulses), respectively. For the temporal characterization of pump and probe pulses cross correlations were measured using the optical Kerr effect [10–12] in, e.g., carbon disulfide. Focussing the two beams on the same spot of a sample (focal diameter ≈100 μm), the transmission changes caused by the pump pulse can be measured with time, frequency and full polarization resolution. Usually signals directly proportional to vibrational population differences are defined by $\Delta\alpha_{||,\perp} = \ln(T_{||,\perp}/T_0)$; the indices refer to the registered probe polarization with respect to that of the pump pulses. In this work only the population dynamics will be studied using the rotation free combination $\Delta\alpha_{rf} = (\Delta\alpha_{||} + 2 \cdot \Delta\alpha_{\perp})/3$. Due to the absorbed pump energy the excited sample volume will end at an elevated temperature level when the vibrational energy is relaxed. The corresponding transmission changes due to thermal modifications of absorption bands of course have to be regarded in $\Delta\alpha_{rf}$. To avoid accumulation of heat, the sample is continuously moved within the focal plane to have a fresh portion of the sample for each laser shot.

3. Results and discussion

We start the presentation of experimental results with two conventional FTIR spectra of a sample of acetic acid in CCl_4 at two different temperatures (298 and 358 K) as given in Fig. 1. The actual concentration was 0.5 mol l^{-1}, but within a range from 0.1 to 2.0 mol l^{-1} the observed quite broad and significantly structured spectral

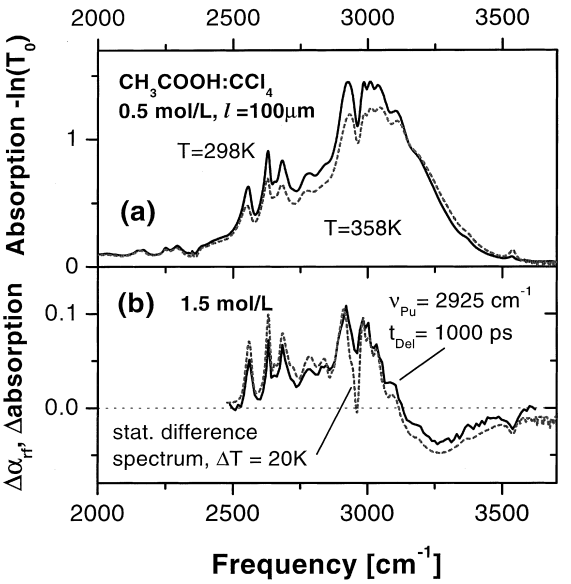

Fig. 1. (a) FTIR spectra of 0.5 mol l^{-1} $CH_3COOH:CCl_4$ at two different temperatures (upper curve: 298 K, lower curve: 358 K); (b) transient spectrum after 1 ns (solid line), and difference of FTIR spectra recorded at 45°C and 25°C (dashed line), concentration 1.5 mol l^{-1}.

bandshape is identical to that given in the figure, only the total absorption strength changes proportional to concentration. The spectral assignment of the various peaks is not unique in the literature (mostly dealing with acetic acid dimers in the gas phase [1,4,5] or solid noble gas matrices at low temperatures [3]), but some general statements are common to all previous investigations: (i) the O–H stretching vibration ν(OH) is strongly redshifted by ~600 cm^{-1} (here most probably the peak at 2930 cm^{-1} represents this mode) due to the rather strong hydrogen bonds in the dimer ring, (ii) the peak at 2580 cm^{-1} is assigned to the overtone of the C–O–H bending mode, whose infrared activity is strongly enhanced by Fermi resonance with ν(OH), and (iii) most of the other peaks observed are caused by coupling to low-frequency modes such as in-plane and out-of-plane ring deformations and the O...O vibration (hydrogen bond stretching). The small peak at 3538 cm^{-1} can be attributed to free OH endgroups [13,14]. The CH_3 stretching vibrations of the methyl group are usually assumed not to be responsible for any of the stronger peaks within the band; this assumption is

plausible comparing, e.g., the situation with a solution of 0.5 mol l^{-1} methanol in CCl_4, which yields a maximum absorption of $-\ln(T_0) \approx 0.5$ in the C–H stretching region around 3000 cm^{-1}. Another hint confirming this assumption is given by the Raman spectrum [15], where the strongest CH_3 peak is observed at 2944 cm^{-1}, i.e., does not coincide with one of the maxima seen in Fig. 1.

The qualitative assignment given above is confirmed by the temperature dependence of the acetic acid spectrum: first, the absorption at 3538 cm^{-1} grows with increasing temperature as would be expected due to an increasing number of free OH endgroups. Second, at higher temperature (lower curve in Fig. 1) the four peaks between 2500 and 2850 cm^{-1} are slightly red-shifted, while those above 2900 cm^{-1} shift to higher frequencies. Such a behavior is quite typical for the different reaction of bending and stretching vibrations to weakening of the hydrogen bonds they are involved in [16,17].

In Fig. 1b a difference of conventional IR spectra of 1.5 mol l^{-1} acetic acid in carbon tetrachloride measured at 45°C and 25°C, respectively (dashed curve), is compared with transient spectral changes obtained 1000 ps after excitation at 2925 cm^{-1} (solid curve); at this time, definitely any vibrational population has relaxed and thermalized. Qualitatively, the two spectra look very similar, but by no means identical; in particular, the most considerable difference, a notch around 2960 cm^{-1} observed in the stationary difference spectrum, indicates that the system is still not in thermodynamic equilibrium after 1 ns. The slightly smaller amplitudes on an average of bleaching and induced absorption in the transient spectrum indicate a laser induced temperature rise below 20 K. It should be noted that a peak of induced absorption at ≈3530 cm^{-1} is present in both spectra indicating an increased number of free OH endgroups.

Fig. 2 presents a selection of transient spectral data obtained on the same sample. First, Fig. 2a compares three spectra recorded after excitation at 2925 cm^{-1} at very early delay times. It is important to note that even at the earliest time there is not only bleaching around the pump frequency, but also at various other positions matching very well the peaks observed in the conventional IR spectrum. With increasing time (and pump intensity) the total amplitude increases, and obviously the relative amplitudes of the not directly pumped peaks grow as compared with the bleaching band at the pump frequency. Additionally a broad induced absorption comes up at frequencies above 3130 cm^{-1}, while at $t_{Del} = -3$ ps there is not yet an absorption change within experimental accuracy. However, at none of these early delay times is an induced absorption present around 3530 cm^{-1} as it was observed in Fig. 1b.

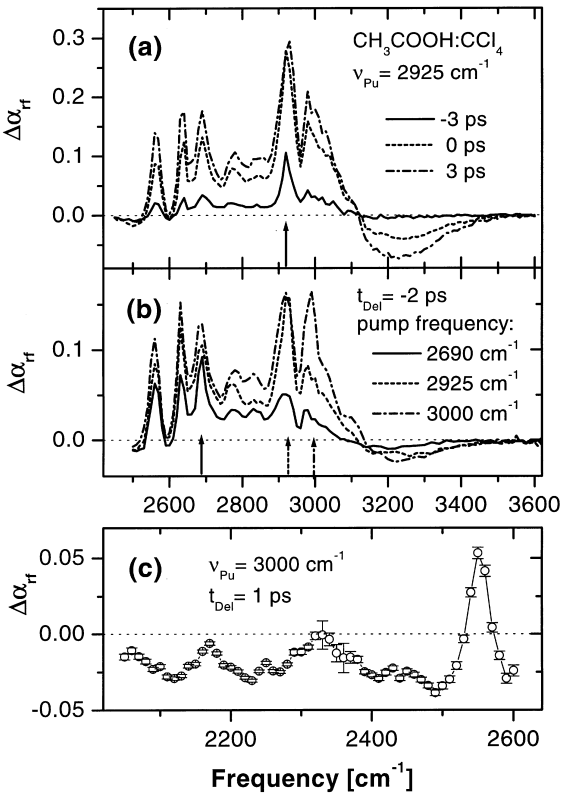

Fig. 2. Spectral results obtained on 1.5 mol l^{-1} $CH_3COOH:CCl_4$: (a) transient spectra at three different delay times, pump frequency 2925 cm^{-1}; (b) transient spectra at three different pump frequencies, delay time −2 ps; (c) transient spectrum in the low-frequency region, pump frequency 3000 cm^{-1}.

In Fig. 2b three spectra recorded at the same early delay time of −2 ps, but with different pump frequencies are presented. It is interesting to observe that in each case again bleaching is observed in the whole spectral range between 2550 and 3100

cm^{-1}, but with considerably different amplitude distribution. Calculating the first spectral moment in this region yields frequency values of 2777 cm^{-1} ($\nu_{pu} = 2690$ cm^{-1}), 2813 cm^{-1} ($\nu_{pu} = 2925$ cm^{-1}) and 2825 cm^{-1} ($\nu_{pu} = 3000$ cm^{-1}), i.e., the 'center frequency' is clearly correlated with the excitation frequency. However, quite obviously the situation cannot be discussed in the usual terms of transient spectral hole burning, in particular because contributions from a coherent coupling artifact at the pump frequency [18,19] cannot be excluded.

Finally Fig. 2c gives the low frequency region down to 2000 cm^{-1} for a delay time of 1 ps, where the maximum amplitude of the induced absorptions was observed in this spectral region. This spectrum was recorded separately due to the change to $AgGaS_2$ crystals and the necessary realignment of the probe beam; in the region around 2350 cm^{-1} the atmospheric CO_2 absorption caused larger uncertainties. The induced absorption seen between 2000 and 2520 cm^{-1} is rather weak, but clearly consists of several separate bands. Because of this distinct structure resembling that of the bleaching region and their frequency positions these induced absorptions can be attributed to excited state absorptions (ESAs) of the O–H stretch band. There may be additional ESAs at higher frequencies, which cannot be resolved due to the overlapping bleaching in this region. Thus an unambiguous assignment of the individual bands and the determination of an anharmonic shift are not possible at present. In contrast to this low-frequency region, the broad blue-shifted induced absorption seen in Fig. 2a is most likely caused by O–H groups in the ν(OH) ground state, whose transition frequency is blue-shifted due to a modified hydrogen bond situation.

More details about the dynamical behavior of the investigated system are revealed by a selection of time resolved data, which are presented in Fig. 3. It should be mentioned that any of the three pump frequencies 2925, 3000 and 3060 cm^{-1} yielded nearly identical results as those shown exemplarily in the figure. An example for an excited state absorption is given in Fig. 3a, which refers to a pump frequency of 3000 cm^{-1} and a probe frequency of 2120 cm^{-1}. The signal decays rather fast, but obviously with a finite decay time. A numerical

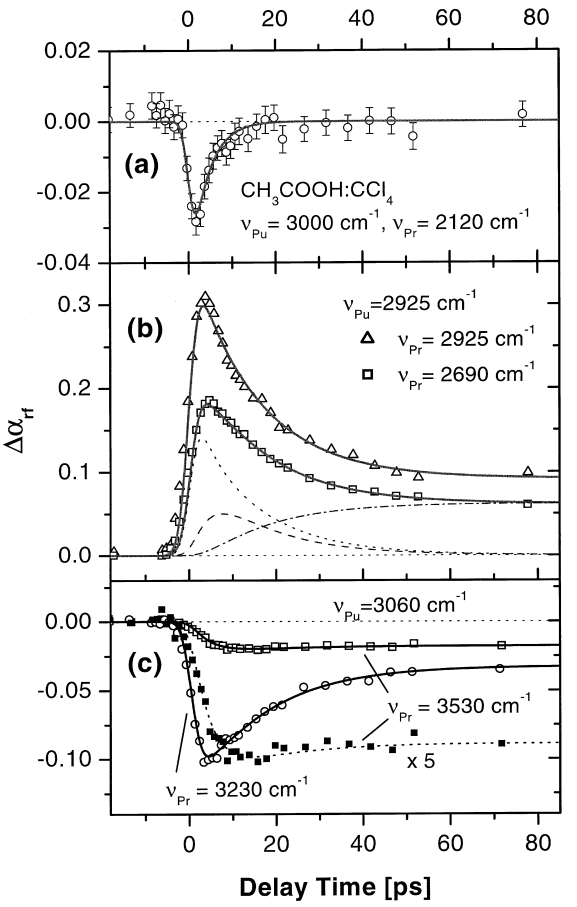

Fig. 3. Time resolved data at several pump/probe combinations (symbols) and numerical simulations (solid curves); the broken curves in (b) refer to the three components of the lower fit curve; in (c) the data at probe frequency 3530 cm^{-1} were multiplied by a factor of 5 for better comparison (data: open squares; fit: dashed line).

simulation assuming single exponential decay (see below) yields a time constant of 4.0 ± 1.5 ps. For the other excited state absorptions in the range 2000–2500 cm^{-1} the same decay time is found within experimental accuracy. The next two curves (Fig. 3b) demonstrate the behavior within the bleaching band: the upper curve (triangles) refers to pump and probe frequency of 2925 cm^{-1}, the lower one (squares) was recorded using the same excitation frequency, but a different probe position (2690 cm^{-1}). Both signals do not return to transmission change zero, but evolve into a constant transmission increase, an observation which is

fully compatible with the long-time spectrum of e.g., Fig. 2c. This constant thermal effect is reached by a considerably slow decay in both cases. At early times, there is a significant difference: probing at the pump frequency, the maximum is reached typically 1 ps earlier as in the case of measuring at a different probe position. Fig. 3c finally shows the time dependence of the blue-shifted induced absorption at two characteristic positions, namely at 3230 cm^{-1} (circles) and at 3530 cm^{-1} (solid squares; original data scaled by a factor of 5 for better visibility), the position of the free O–H groups. Both curves rise to a maximum and then decay back to a constant value, but clearly the curve measured at 3530 cm^{-1} shows a slower rise time and a much less pronounced overshoot.

Analyzing the observations from both spectral and time-resolved data several qualitative conclusions can be drawn: the occurrence of the structured, strongly red-shifted excited state absorption clearly proves the presence of a considerable amount of vibrational population at early times as well as a fast redistribution among the various modes within the dimer ring system. The latter is confirmed by the nearly simultaneous bleaching of several peaks between 2570 and 3100 cm^{-1}; as here also the ground state population is probed, this result indicates a fast redistribution within the depleted ground state as well. Also the observation of very similar results using different pump frequencies is a hint in this direction. The time constant of the redistribution process seems to be finite, i.e., slower than ≈100 fs, because otherwise neither the changes with increasing delay time observed in Fig. 2a nor the differences between different pump frequencies seen in Fig. 2b could be observed with our current time resolution. The whole vibrational ensemble then relaxes with a time constant of approximately 4 ps. No indication for a long-lived intermediate vibrational mode was found in agreement with results reported previously [8]. All induced absorption at $\nu >$ 3130 cm^{-1} is obviously caused by OH groups, the hydrogen bonds of which are weakened (leading to the broad induced absorption) or even broken (narrow band at ≈3530 cm^{-1}). The blue-shift of the dimer OH band due to weakened hydrogen bonds can be caused by coupling to excited low-frequency ring modes of the dimer as well as by already relaxed excess energy in the immediate surroundings of the initially excited molecules, i.e., roughly speaking by a high 'local temperature'. The occurrence of free OH groups could be either a relaxation channel itself ('vibrational predissociation') or a reaction to the increased temperature. Finally the relaxed energy will be really thermalized, i.e., distributed among the whole focal volume. This situation is reached within ≈100 ps producing the transmission changes observed at later delay times, and then remains constant for the whole delay range (4 ns) of our experiment.

For a more detailed analysis and, in particular, to extract the involved time constants, rate equation based numerical simulations were performed. According to the above qualitative findings, a suitable model has to account for at least the following steps after vibrational excitation: (i) redistribution of vibrational energy, (ii) relaxation of the vibrational ensemble, (iii) transmission changes due to already thermalized energy in the surroundings of the initially excited molecules, and (iv) evolution of these thermal transmission changes with thermal equilibration within the whole focal volume. The following, strongly simplified rate equation model meets these requirements and turned out to be sufficient to fit all available data: the initial excitation step populates a vibrational level (1); the redistribution among the variety of modes within the broad O–H dimer band is substituted by redistribution with a time constant τ_{red} to another single level (2) only (of course regarding 'detailed balance'); the inclusion of additional levels of this type did not change the fit quality measurably, most probably because the bleaching contribution due to ground state depletion in this case dominates the signal anyhow. These two levels are assumed to lose their vibrational population with a common effective lifetime T_1 (i.e., in the model both levels are assigned a relaxation channel with rate constant $1/T_1$). This relaxation step is assumed to end at a third, intermediate level (3); this level is interpreted as a modified, 'hot' ground state, i.e., the initial vibrational energy is assumed to have been transferred to 'thermal' energy (translation, rotation, low-en-

ergy vibrations) of the dimer itself or the immediately neighboring solvent molecules. Spectroscopically, this effect means a (strong) modification of the absorption of the initially excited molecules; in the simulation of the data this level can lead to positive (bleaching) or negative (induced absorption) contributions, depending on the probe frequency. Finally, the system is assumed to come back to its ground state with a thermal time constant τ_{th}; in this step the amount of relaxed energy is registered, and a thermal effect (bleaching or induced absorption) being proportional to this amount of relaxed energy is introduced. Physically, this step describes the thermalization process (heat diffusion) of the relaxed energy within the focal volume; at the end of this step all acetic acid molecules within the focal volume are assumed to have the same average temperature, and thus contribute to the long-time spectral changes, which then remain constant for several nanoseconds.

Using this model, the best fits to the current data (represented by the solid curves in Fig. 2) were obtained with the parameters $\tau_{red} = 500 \pm 300$ fs, $T_1 = 4 \pm 1.5$ ps, $\tau_{th} = 15 \pm 2$ ps (using identical pump and probe pulse duration of 2.7 ps). The following contributions had to be regarded to compose the individual curves: (i) for the data of Fig. 2a only an excited state absorption starting from level (1) was needed; (ii) in Fig. 2b, both curves consist of three components (given as broken lines for the lower curve in the figure), namely the appropriate fundamental transition ($0 \rightarrow 1$ or $0 \rightarrow 2$, respectively), a bleaching component proportional to the 'population' in level (3), and the long-time thermal effect; (iii) in Fig. 2c, the upper curve (at the position of free O–H groups) could be explained by induced absorption proportional to level (3) plus thermal effect, while the data measured at 3230 cm^{-1} additionally required a fast component to explain the signal rise; in the simulation an induced absorption proportional to population on level (2) was used to account for this.

In general these results confirm the conclusions made directly from the data; in particular it seems clear that there is a modification of the O–H absorption band already at very early times, i.e., during vibrational relaxation, leading to bleaching of the original absorption and the broad blue-shifted induced absorption. So possibly even the excitation of low-energy vibrations within the ring system due the strong coupling of the various modes already changes the absorption spectrum. In contrast to this, the free O–H groups occur typically with the same time constant as the vibrational population decreases. So for the case of acetic acid dimers it cannot be decided if vibrational predissociation is an effective relaxation channel itself, or if hydrogen bond breaking is dominatingly a thermally activated process. However, an important hint to the dominating process can be derived from recent studies of an alcohol dimer with only a single hydrogen bond, which shows time scales for the lifetime of the OH stretching vibration [20] and the energy migration along the hydrogen bond [21] very similar to those observed in our work. In particular, although the hydrogen bond of the alcohol dimer is considerably weaker than in the case of acetic acid, no indication of vibrational predissociation has been found there. In a different study it was shown that even conservation of vibrational energy during dimer formation via hydrogen bonding is possible [22]. So it is quite reasonable to favor thermal bond breaking for the case of acetic acid dimers, too. The fast thermalization of the relaxing vibrational energy needed for this assumption is also very plausible, since the low-frequency modes within the dimer ring should be able to effectively transfer energy to the thermal bath of the solvent.

In our above described model, it was assumed that the slowest decay time observed in our experiments (15 ps) refers to nanoscopic heat diffusion, i.e., the transfer of relaxed energy from the immediate surroundings of initially excited acetic acid molecules to those which were not vibrationally excited. The plausibility of this idea was checked solving numerically the (macroscopic) heat conduction equation for the spherically symmetric problem of an isolated 'hot spot' in approximation of the initially excited dimer (an initial Gaussian temperature profile was used). Calculating for this situation the temporal dependence of the temperature at radial distances between 0.5 and 3.5 nm (the latter is the average distance of vibrationally excited acetic acid

molecules in our samples assuming an overall excitation of 5%) yields temperature variations on time scales between ≈2 and several 10 ps. As the real situation is a rather complicated superposition of such individual results, it is quite plausible that the average gives a nearly exponential decay with an intermediate time constant. This finding can be taken as a significant hint to interpret the signal decay with 15 ps as to be mainly due to nanoscopic heat diffusion and, probably, the rearrangement of the hydrogen bonds as a reaction to the temperature change. When these processes are finished, the thermal transmission changes observed at delay times >100 ps are established. This situation is physically only a quasi-equilibrium, since the hot focal volume must lead to successive processes like volume expansion or heat diffusion out of the focal volume; these processes however are known to happen on vastly slower time scales [23]. On this background it is quite reasonable that the transient spectral changes at late delay times and conventional temperature difference spectra are very similar, but not really identical due to, e.g., the pressure increase within the focal volume [23].

In summary, using infrared double resonance spectroscopy we have found a fast, subpicosecond redistribution of vibrational energy within the very broad OH band of acetic acid dimers and an effective vibrational lifetime of 4 ps for this manifold of modes. An additionally observed slower decay with a time constant of 15 ps is attributed to the effects of thermalization and nanoscopic heat diffusion within the focal volume. It will be an interesting aspect of future work to study these phenomena in more detail varying, e.g., sample temperature and concentration.

References

[1] Y. Maréchal, A. Witkowski, J. Chem. Phys. 48 (1968) 3697.
[2] O.N. Nielsen, P.-A. Lund, J. Chem. Phys. 78 (1983) 652.
[3] R.L. Redington, K.C. Lin, J. Chem. Phys. 54 (1971) 4111.
[4] Y. Marechal, J. Chem. Phys. 87 (1987) 6344.
[5] K. Fukushima, B. Zwolinski, J. Chem. Phys. 50 (1969) 737.
[6] L. Turi, J.J. Dannenberg, J. Phys. Chem. 97 (1993) 12197.
[7] L. Turi, J. Phys. Chem. 100 (1996) 11285.
[8] M. Bonn, S. Woutersen, H.J. Bakker, Opt. Commun. 147 (1998) 138.
[9] K. Wolfrum, J. Löbau, W. Birkholzer, A. Laubereau, Quantum Semiclass. Opt. 9 (1997) 257.
[10] G. Seifert, H. Graener, Bull. Pol. Acad. Sci. Chem. 47 (1999) 397.
[11] G. Seifert, T. Patzlaff, H. Graener, Vibr. Spectrosc. 23 (2000) 219.
[12] G. Seifert, H. Graener, Opt. Commun. 115 (1995) 216.
[13] C.V. Berney, R.L. Redington, K.C. Lin, J. Chem. Phys. 53 (1970) 1713.
[14] E.V. Stefanovich, T.N. Truong, J. Chem. Phys. 105 (1996) 2961.
[15] B. Schrader, Raman/Infrared Atlas of Organic Compounds, VCH, Weinheim, 1989.
[16] D. Hadzi, S. Bratos, in: P. Schuster, G. Zundel, C. Sandorfy (Eds.), The Hydrogen Bond, vol. II, North-Holland, Amsterdam, 1976, 565pp.
[17] H. Graener, G. Seifert, A. Laubereau, Chem. Phys. 175 (1993) 193.
[18] R. Laenen, C. Rauscher, Chem. Phys. 230 (1998) 223.
[19] S. Woutersen, H.J. Bakker, J. Opt. Soc. Am. 17 (2000) 832.
[20] R. Laenen, K. Simeonidis, J. Phys. Chem. A 102 (1998) 7207.
[21] R. Laenen, K. Simeonidis, Chem. Phys. Lett. 292 (1998) 631.
[22] S.M. Arrivo, E.J. Heilweil, J. Phys. Chem. 100 (1996) 11975.
[23] H. Graener, R. Zürl, M. Bartel, G. Seifert, J. Mol. Liquids 84 (2000) 161.